J Appl Electrochem (2009) 39:1399–1407
DOI 10.1007/s10800-009-9810-9

ORIGINAL PAPER

Synergistic effect of iodide ions on inhibitive performance of 2,5-bis(4-methoxyphenyl)-1,3,4-thiadiazole during corrosion of mild steel in 0.5 M sulfuric acid solution

Fouad Bentiss · Mounim Lebrini · Michel Traisnel · Michel Lagrenée

Received: 24 April 2008 / Accepted: 27 January 2009 / Published online: 17 February 2009

Abstract The synergistic effect of iodide ions on the corrosion inhibition of mild steel in 0.5 M H_2SO_4 solutions by 2,5-bis(4-methoxyphenyl)-1,3,4-thiadiazole (4-MTH) has been studied using electrochemical impedance spectroscopy (EIS) and the Tafel polarisation method. The results showed that the inhibition efficiency increased with 4-MTH concentration while the potential of desorption (E_d) remained unchanged. The addition of potassium iodide (KI) in the acid solution stabilized the adsorption of 4-MTH molecules on the metal surfaces and, therefore, enhanced the inhibition efficiency of 4-MTH and increased the value of E_d. The synergistic effect was observed between KI and 4-MTH with an optimum mass ratio of [4-MTH]/[KI] = 5/5. The calculated values of synergism parameter (S_θ) from the coverage of the surface were found to be more than unity in most cases. This clearly showed the synergistic influence of iodide ions on the corrosion inhibition of mild steel in 0.5 M H_2SO_4 by 4-MTH. The adsorption of this inhibitor alone and in combination with iodide ions followed Langmuir's adsorption isotherm.

F. Bentiss (✉)
Laboratoire de Chimie de Coordination et d'Analytique, Faculté des Sciences, Université Chouaib Doukkali, B.P. 20, 24000 El Jadida, Morocco
e-mail: fbentiss@enscl.fr

M. Lebrini · M. Traisnel
Laboratoire des Procédés d'Elaboration des Revêtements Fonctionnels, PERF-LSPES UMR-CNRS 8008, ENSCL, BP 90108, 59652 Villeneuve d'Ascq Cedex, France

M. Lagrenée (✉)
Unité de Catalyse et de Chimie du Solide, UMR-CNRS 8181, ENSCL, BP 90108, 59652 Villeneuve d'Ascq Cedex, France
e-mail: michel.lagrenee@ensc-lille.fr

Keywords Thiadiazole · Acid corrosion inhibitor · Mild steel · Synergistic effect · Halide ions · Adsorption · Tafel polarisation

1 Introduction

Acid solutions are widely used in many industrial processes. Hydrochloric acid, phosphoric acid and sulfuric acid are aggressive solutions used for acid picking, acid cleaning and acid descaling due to their special chemical properties. The use of corrosion inhibitors is one of the most practical methods for metal corrosion protection. Corrosion inhibitors can be used to prevent metal from corrosion in aggressive media [1–6]. Generally studies on corrosion inhibitors mainly focus on three domains: first we have to find the appropriate inhibitor among the known compounds, next, we have to synthesize new compounds under the direction of theoretical calculation, and the last step is identify synergistic actions among various compounds to expand the range of inhibitor application.

Synergistic effects describe an increase in effectiveness of the corrosion inhibitor in the presence of another substance in the corrosive medium. The role of synergism on the corrosion inhibition mechanism of steel in acidic solutions has been reported by several authors [7–16]. Some researchers [17–22] found that nitrogen containing organic compounds are more effective for the steel corrosion inhibition in hydrochloric acid than in sulfuric acid. The possible reason is that there is a synergistic effect between chloride ions and nitrogen containing organic compounds for steel corrosion in hydrochloric acid.

The aim of the present study is to investigate the synergistic influence of iodide ions on the performance of 2,5-bis(4-methoxyphenyl)-1,3,4-thiadiazole (4-MTH) as a

corrosion inhibitor model compound in 0.5 M sulphuric acid solution using electrochemical methods.

2 Experimental detail

The tested inhibitor, namely 2,5-bis(4-methoxyphenyl)-1,3,4-thiadiazole (4-MTH) was synthesised according to a previously described procedure [23]. The molecular structure of 4-MTH is shown in Fig. 1. The concentration range employed was 0.25 × 10 to 1.5 × 10^{-4} M. Corrosion tests were carried out on electrodes cut from sheets of mild steel. Steel strips containing 0.09% P, 0.38% Si, 0.01% Al, 0.05% Mn, 0.21% C, 0.05% S and the remainder iron were used for the measurement of weight loss and for electrochemical studies. The surface preparation of the specimens was carried out using emery paper grade 600 and 1,200; they were degreased with ethanol under ultrasound and dried at room temperature before use. The solutions (0.5 M H_2SO_4) were prepared by dilution of analytical reagent grade sulphuric acid (96%) with bidistilled water.

Gravimetric experiments were carried out in a double glass cell equipped with a thermostated cooling condenser. The solution volume was 100 mL. The steel specimens used had rectangular form (length = 2 cm, width = 1 cm, thickness = 0.06 cm). Experiments were performed at 30 °C for 24 h immersion in aerated acid solutions. After the exposure time, the specimens were taken out, carefully rinsed with bi-distilled water, ultrasonically cleaned in ethanol and then weighed. The experiments were done in duplicate and the average value of the weight loss was reported.

Electrochemical impedance spectroscopy (EIS) and polarisation curves were conducted at 30 ± 1 °C using an electrochemical measurement system (Tacussel-Radiometer PGZ 301). Electrochemical experiments were carried out in a glass cell with a capacity of 500 mL for polarisation curves and a polymethyl methacrylate (PMMA) cell with a capacity of 1,000 mL for AC impedance measurements. A saturated calomel electrode (SCE) was used as reference; a Pt electrode was used as counter electrode. All potentials are reported versus SCE.

For Tafel polarisation experiments the working electrode was prepared from a cylindrical mild steel rod insulated with polytetrafluoethylene tape (PTFE) so that the area exposed to solution was 1 cm^2. A fine Luggin capillary was placed close to the working electrode to minimize ohmic resistance. All the tested solutions were de-aerated in the cell by using pure nitrogen for 30 min prior to the experiment. During each experiment the tested solution was mixed with a magnetic stirrer and gas bubbling was maintained. The procedure adopted for the polarisation measurements was the same as previously described [24]. The anodic and cathodic polarisation curves were recorded at a constant sweep rate of 0.5 mV s^{-1}.

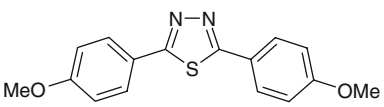

Fig. 1 Molecular structure of 1,3,4-thiadiazole (4-MTH)

AC impedance measurements were performed after 24 h immersion using a Tacussel Radiometer PGZ 301 Frequency Response Analyser in the frequency range 10^5–10^{-2} Hz with ten points per decade. An ac sinusoid ±10 mV was applied at the corrosion potential (E_{corr}). The experiments were carried out under static conditions at 30 ± 1 °C in aerated acid solutions. The working electrode was prepared from a square sheet of mild steel so that the area exposed to solution was 7.55 cm^2. The impedance data were analysed and fitted using graphing and analysing impedance software (version Voltamaster 4). Nyquist plots were made from these experiments. The best semicircle was fitted through the data points in the Nyquist plot using a non-linear least squares fit to give the intersections with the *x*-axis [25].

3 Results and discussion

3.1 Inhibition of acid corrosion by 4-MTH

3.1.1 Comparative study in 1 M HCl and 0.5 M H_2SO_4

The addition effect of 4-MTH at different concentrations on mild steel corrosion in 1 M HCl and 0.5 M H_2SO_4 solutions was studied by weight loss at 30 °C after 24 h of immersion. The inhibition efficiency $E(\%)$ was calculated as previously described [26]. The calculated values of corrosion rate (W_{corr}) and $E(\%)$ are given in Table 1. Corrosion rate decreases with increase in inhibitor concentration while $E(\%)$ values increase with increase in 4-MTH concentration (Table 1). The inhibition efficiencies in the case of hydrochloric acid show the same trend as those previously obtained from AC impedance studies [27]. At the highest inhibitor concentration, 1.5 × 10^{-4} M, the inhibition efficiency attains 98% in 1 M HCl and only 76.5% in 0.5 M H_2SO_4 (Table 1). This result is best explained in terms of adsorbability of Cl^- and SO_4^{2-} [28]. Adsorption of organic molecules is not always a direct combination of the organic molecules with the metal surface [29]. In some cases, the adsorption occurs through the already adsorbed chloride or sulphate ions which interfere with the adsorbed organic molecules [30]. Indeed, the specific adsorption of anions is expected to be more

Table 1 Calculated values of inhibition efficiency and corrosion rate for mild steel in 1 M HCl and in 0.5 M H_2SO_4 without and with 4-MTH after 24 h of immersion at 30 °C obtained from weight loss measurements

Acid solution	Concentration (10^{-4} M)	W_{corr} (mg cm^{-2} h^{-1})	E (%)
1 M HCl	0	1.2877	–
	0.25	0.0835	93.5
	0.5	0.0764	94.1
	1.0	0.0595	95.4
	1.5	0.0262	98.0
0.5 M H_2SO_4	0	1.6612	–
	0.25	1.0566	36.5
	0.5	0.6537	60.7
	1.0	0.5171	68.9
	1.5	0.3899	76.5

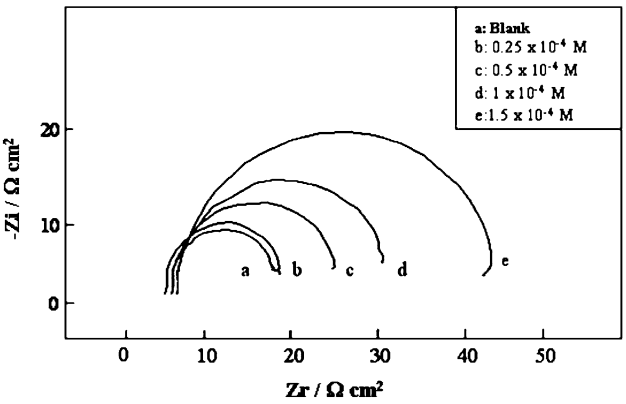

Fig. 2 Nyquist diagrams for mild steel in 0.5 M H_2SO_4 containing different concentrations of 4-MTH

Table 2 Impedance parameters for the corrosion of mild steel in 0.5 M H_2SO_4 without and with 4-MTH after 24 h of immersion at 30 °C

Inhibitor conc. (M)	R_t (Ω cm^2)	C_{dl} (μF cm^{-2})	$E_{rest\ potential}$ (mV_{SCE})	E (%)
Blank	9	1,782	−492	–
0.25×10^{-4}	14	834	−468	35.7
0.5×10^{-4}	22	506	−471	59.1
1.0×10^{-4}	28	480	−465	67.9
1.5×10^{-4}	40	352	−473	77.5

pronounced with anions having a smaller degree of hydration, such as chloride ions. Being specifically adsorbed, they create an excess of negative charge towards the solution phase and favour more adsorption of thiadiazole cations, leading to greater inhibition [31].

In order to improve the protective properties of 4-MTH in 0.5 M H_2SO_4 medium, the synergistic effect between halide-ions, particularly iodide ions, was investigated using ac and dc electrochemical techniques.

3.1.2 *Influence of 4-MTH concentration in 0.5 M H_2SO_4 solution*

The corrosion behaviour of mild steel in 0.5 M H_2SO_4 solution in the absence and presence of 4-MTH was also investigated by electrochemical impedance spectroscopy (EIS) at 30 °C after 24 h of immersion. Nyquist plots of mild steel in uninhibited and inhibited acidic solutions containing various concentrations of 4-MTH are given in Fig. 2. The impedance response of mild steel in uninhibited 0.5 M H_2SO_4 solution changes significantly after thiadiazole addition. The results can be interpreted in terms of the equivalent circuit of the electrical double layer as previously described [32]. Nyquist plots (Fig. 2) are depressed into the real axis and are not perfect semi-circles as a result of the roughness and other non-homogeneities of the metal surface [33, 34]. This phenomenon is known as the "dispersing effect" [35]. The impedance parameters deduced from the analysis of Nyquist diagram and values of E(%) are given in Table 2. Double layer capacitance values (C_{dl}) and charge-transfer resistance values (R_t) were obtained from impedance measurements as previously described [36]. In the case of the AC impedance study, the inhibition efficiency E(%) is calculated by charge transfer resistance as previously described [37]. With increasing inhibitor concentration, the R_t value increases and the inhibiting power becomes higher (Table 2). A large charge-transfer resistance is associated with a slower corroding system. Furthermore, better protection provided by an inhibitor can be associated with a decrease in capacitance. The decrease in the C_{dl}, which results from a decrease in local dielectric constant and/or an increase in the thickness of the electrical double layer, suggests that the 4-MTH molecules function by adsorption at the metal solution/interface [32]. However, the effectiveness of 4-MTH does not exceed 77.5% at maximum concentration of 1.5×10^{-4} M in normal sulphuric medium. The AC impedance study confirms the conclusion of the gravimetric tests, giving some additional information about the type of inhibition in 0.5 M H_2SO_4.

Figure 3 shows the anodic and cathodic polarisation curves recorded on mild steel in 0.5 M H_2SO_4 solution in the presence and absence of 4-MTH. As expected, both anodic and cathodic currents were inhibited with increase in inhibitor concentration. This suggests that the addition of the investigated 1,3,4-thiadiazole reduces anodic dissolution and also retards the hydrogen evolution reaction, indicating that this inhibitor exhibits cathodic and anodic inhibition effects [26]. Therefore, 4-MTH can be classified

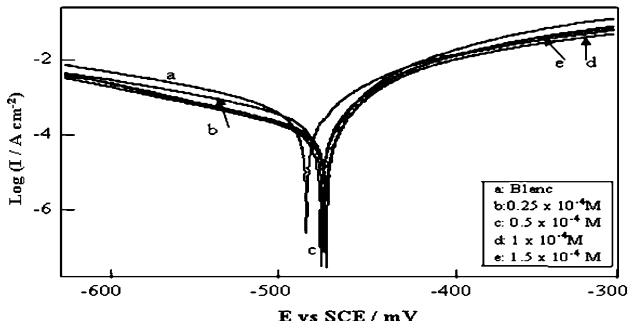

Fig. 3 Polarisation curves for mild steel in 0.5 M H_2SO_4 containing different concentrations of 4-MTH

as an inhibitor of relatively mixed effect in 0.5 M H_2SO_4. Cathodic current potential curves give rise to parallel Tafel lines (Fig. 3) indicating that the hydrogen evolution reaction is activation controlled and the addition of 4-MTH does not affect the mechanism of the proton discharge reaction [26]. In the anodic domain, two linear portions were observed on the anodic polarization curves in the presence of 4-MTH (Fig. 3). With increase in anodic potential, the anodic currents increase with a first anodic slope (b_{a1}) in the low polarization potential region. After passing a certain potential (>−430 mV_{SCE}), the anodic currents increase and dissolution occurs at a second anodic slope (b_{a2}) in the high polarization potential region. The corresponding mechanism has been proposed elsewhere [38, 39]. In the present work, the rapid increase of anodic current at the second polarization region may be due to desorption of 4-MTH molecules. In this case, the desorption rate of thiadiazole is higher than its adsorption rate [40]. The potential values related to the intersection of the two linear portions, characterized by two anodic slopes, are called the potential of desorption (E_d) [40, 41]. The value of E_d indicates the beginning of the absorbed species desorption on the electrode surface. Over this value, the coverage of the inhibitor decreases rapidly.

Electrochemical corrosion kinetic parameters, such as corrosion potential (E_{corr}) and corrosion current density (I_{corr}) are presented in Table 3. These values were obtained by extrapolation of the Tafel slopes for the studied thiadiazole at the evaluated concentrations. $E(\%)$ is calculated by I_{corr} as previously described [24]. As expected, the $E(\%)$ values increased with increasing inhibitor concentration, reaching a maximum value at 1.5×10^{-4} M of 4-MTH (Table 3). The I_{corr} values considerably decreased in the presence of 4-MTH while the E_{corr} values shifted slightly in the positive direction with increase in inhibitor concentration. In addition, the values of E_d remain nearly constant with increase in 4-MTH concentration. This result suggests that the potential of desorption is slightly affected by the 4-MTH coverage.

Table 3 Polarisation parameters of mild steel in 0.5 M H_2SO_4 without and with 4-MTH at 30 °C

Inhibitor conc. (M)	E_{corr} (mV_{SCE})	I_{corr} (μA cm^{-2})	E (%)
Blank	−482	1,540	–
0.25×10^{-4}	−475	1,018	33.9
0.5×10^{-4}	−473	668	56.6
1.0×10^{-4}	−472	527	65.8
1.5×10^{-4}	−470	396	74.3

From these polarisation results, it has been demonstrated that 4-MTH is a relatively effective inhibitor for mild steel in sulphuric acid. However, the potential of desorption, E_d, remains unchanged but the corrosion potential (E_{corr}) changes with the increase in 4-MTH concentration. Therefore, the stability of the adsorbed 4-MTH layer on the metal is the major problem to be addressed for improving thiadiazole inhibition efficiency in 0.5 M H_2SO_4.

3.2 Synergism of halide ions with 4-MTH

3.2.1 Effect of halide ions

The influence of the halide ions on the inhibitive action of 4-MTH in 0.5 M H_2SO_4 solution was investigated by electrochemical impedance spectroscopy (EIS). Figure 4 compares the effect of different halide ions on the impedance behaviour of mild steel in the presence of 4-MTH. With the 4-MTH alone (curve a), the R_t value was found to be around 28 Ω cm^2 and C_{dl} value about 480 μF cm^{-2}, while in presence of combined inhibitor [4-MTH + KCl] (curve c), [4-MTH + KBr] (curve d) and [4-MTH + KI] (curve e), the values of R_t increased considerably to 53, 64 and 90 Ω cm^2, respectively and C_{dl} decreased to 480,1 and 73 μF cm^{-2}, respectively (Fig. 5). These results

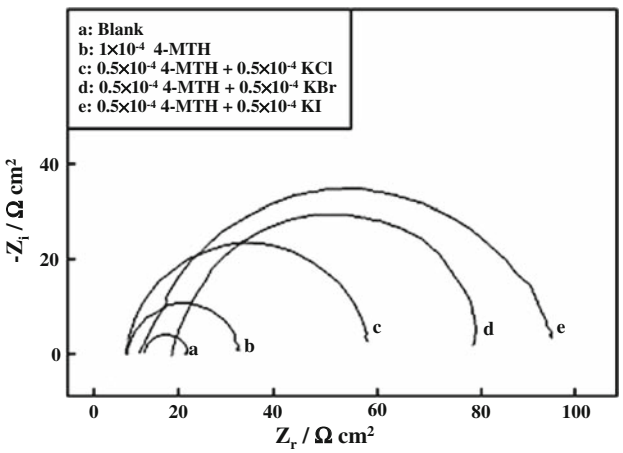

Fig. 4 Effect of different halide ions on the impedance behaviour of mild steel in 0.5 M H_2SO_4 in the presence of 4-MTH

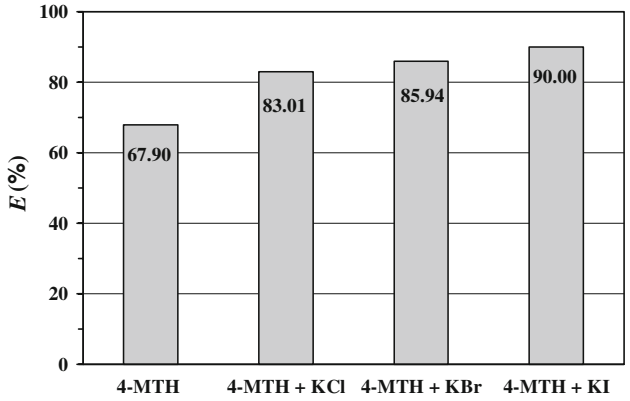

Fig. 5 Variation of inhibition efficiency with different halide ions for mild steel in 0.5 M H_2SO_4 containing 1×10^{-4} M of combined inhibitor ([4-MTH] = [KX], $X = Cl^-$, Br^- and I^-)

demonstrate that there are synergistic effects between 4-MTH and the studied halide ions on the corrosion inhibition of mild steel in the sulphuric acid solutions. This synergistic effect was observed to follow the order $Cl^- < Br^- < I^-$. This conclusion is in accordance with other findings [12, 41, 42]. The large size and the great polarisability of I^- facilitate electron pair bonding and therefore enhances the inhibiting power [43]. Thus, I^- is the most effective halide ion to be used together with the investigated 1,3,4-thiadiazole.

Antropov et al. [44] explain the increase in the adsorption degree of organic cations in the presence of halide ions by electrostatic interactions between the adsorbed species. According to Iofa [45], the anions adsorbed on the metal surface form interconnecting bridges between the metal atoms and the organic cations and thus facilitate cation adsorption.

The position of the potential of zero charge (PZC) can be useful to explain the positive synergistic effect observed in the corrosion inhibition of mild steel in sulphuric acid solutions by organic cations in the presence of halide ions [46, 47]. Thus the AC impedance study was used to evaluate the potential of zero charge (PZC) from the capacitance (C_{dl}) versus voltage (E) plot [48]. In order to gain more information about the adsorption behaviour of 4-MTH molecules on the steel surface when adding halide ions in 0.5 M H_2SO_4, C_{dl} versus applied potential (E) plots were recorded for steel in 0.5 M H_2SO_4 solutions in the presence of 4-MTH and the combined inhibitor [4-MTH + KI] (Fig. 6). The minima on the C_{dl} versus E curves, considered as the value of PZC of the electrode, are −480 and −500 mV_{SCE} for 4-MTH and the combined inhibitor [4-MTH + KI], respectively. The free corrosion potential values (E_{corr}) of mild steel in 0.5 M H_2SO_4 in the presence of 4-MTH and the combined inhibitor [4-MTH + KI] are −465 and −470 mV_{SCE}, respectively. The surface charge can be defined by the position of the corrosion potential E_{corr} with respect to the PZC. When the difference $\varphi = E_{corr} - E_{q=0}$ is negative, the electrode surface has a negative net charge and the adsorption of cations is favoured. On the contrary, the adsorption of anions is favoured when φ becomes positive [49]. In this work, the corresponding values of φ of mild steel in 0.5 M H_2SO_4 in the presence of 4-MTH and the combined inhibitor [4-MTH + KI] are +15 and +30 mV_{SCE}, respectively. These results indicate that the anions (I^- and/or SO_4^{2-}) ions will first be adsorbed on the metal surface; this in turn will attract the thiadiazole cationic forms and protonated water molecules. So a close-packed triple layer will form on the metal surface and inhibit iron ions from entering the solution. Hence, the increase in the positive charge on the metal surface in the presence of combined inhibitor [4-MTH + KI] compared to 4-MTH alone is mainly due to the presence of iodide ions [50]. It can be concluded that the addition of KI improves the adsorption of 4-MTH and therefore the inhibition efficiency of 4-MTH in 0.5 M H_2SO_4 solution (Fig. 5).

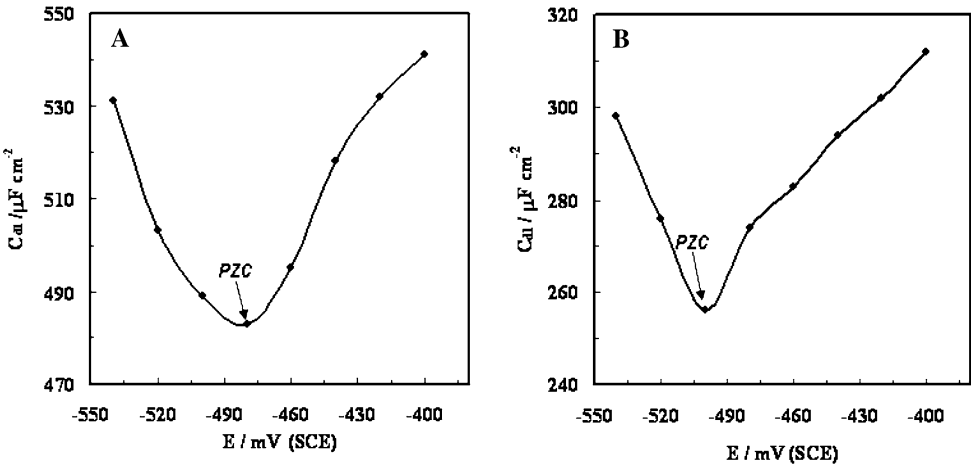

Fig. 6 Capacitance versus voltage plots for mild steel in 0.5 M H_2SO_4 containing **a** 1×10^{-4} M 4-MTH and **b** 1×10^{-4} M (KI + 4-MTH) with [KI] = [4-MTH]

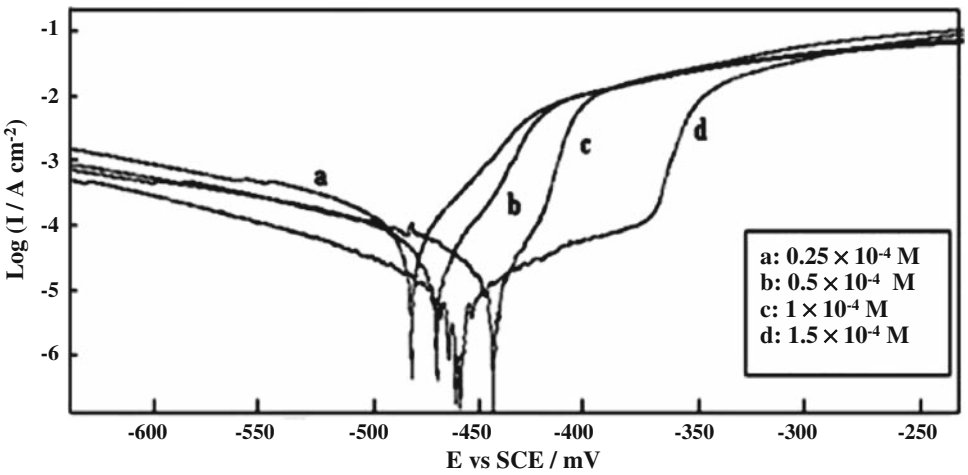

Fig. 7 Polarisation curves for mild steel in 0.5 M H_2SO_4 containing different concentrations of KI

Table 4 Polarisation parameters of mild steel in 0.5 M H_2SO_4 without and with KI at 30 °C

KI conc. (M)	E_{corr} (mV_{SCE})	E_d (mV_{SCE})	I_{corr} (μA cm^{-2})	E (%)
Blank	−482	–	1,540	–
0.25×10^{-4}	−480	−412	862	44.0
0.5×10^{-4}	−470	−406	718	53.4
1.0×10^{-4}	−444	−400	554	64.0
1.5×10^{-4}	−461	−375	450	70.8

3.2.2 *Influence of KI concentration*

Figure 7 shows the polarization curves for mild steel in 0.5 M H_2SO_4 solution in the presence of different concentrations of KI. As expected, the addition of KI decreases the rates of both hydrogen evolution and steel dissolution. The electrochemical parameters from the polarization curves are listed in Table 4. The decrease in corrosion current density (I_{corr}) and positive shift of E_{corr} with increase in KI concentration are similar to that observed for iron in iodide-containing sulphuric acid reported by Heusler and Cartledge [41] and Feng et al. [12]. Besides, the potential of desorption, E_d, was found to be a function of iodide concentration. The E_d values were positively shifted with increasing KI concentration (Table 4). The value of E_d is related to the amount of adsorbed iodide ions on the iron electrode surface, according to the studies of Heusler and Cartledge [41]. The same behaviour is shown in the case of steel.

The addition of potassium iodide to sulphuric acid resulted in a positive shift of the E_d, hence increasing the stability of the adsorbed species on the electrode surface. At the same molar concentration of 1.5×10^{-4} M of either KI or 4-MTH, the E_d value for KI is approximately 55 mV higher than that obtained for 4-MTH. Therefore, KI may be used to improve the adsorption stability of 4-MTH on steel.

3.2.3 *Effect of the mixture 4-MTH with KI*

The Tafel polarization curves were used in order to determine the optimum ratio of 4-MTH and KI. The total concentration of KI and 4-MTH remained constant at 10^{-4} M in all experiments. The corrosion kinetic parameters are tabulated in Table 5. When only KI was added to the solution, the value of I_{corr} was relatively high (554 μA cm^{-2}) and a high value of E_d (−375 mV_{SCE}) was observed. When only 4-MTH was added, the corrosion current density (I_{corr}) was 527 μA cm^{-2} and E_d was relatively low (−430 mV_{SCE}). I_{corr} was reduced to 191 μA cm^{-2} when 5×10^{-5} 4-MTH and 5×10^{-5} KI were used together, indicating that a synergistic effect exists. The synergistic effect between 4-MTH and KI can be explained by the fact that the addition of KI stabilized the adsorption of 4-MTH on the steel surface. Indeed, the increase in E_d values with KI concentration, shown in Table 5, demonstrates the increase in stability of the absorbed 4-MTH layer. However, excessive amounts of KI may result in the occupancy of the limited active sites available for the adsorption of 4-MTH molecules, which are necessary to cover the electrode surface in order to ensure steel protection against the acid corrosion. On the other hand, the addition of 4-MTH in the solutions tends to reduce the E_d values, resulting in an increase in the desorption tendency of the adsorbed I^- ions on the metal surface [12]. The blend inhibitor (4-MTH + KI) combines the advantages of both KI (high E_d) and 4-MTH (high inhibiting power). In addition, the highest E(%) value was calculated at [KI]/[4-MTH] = 5/5 (Fig. 8), suggesting that the optimum ratio is obtained with equal molar concentrations of 4-MTH and KI.

Table 6 gives the electrochemical parameters obtained from polarization cures for mild steel in 0.5 M sulphuric acid in the presence of different concentrations of the combined inhibitor (4-MTH + KI) in equal molar

Table 5 Polarisation parameters of mild steel in 0.5 M H_2SO_4 containing 1×10^{-4} M (4-MTH + KI) with different ratios of 4-MTH and KI concentrations at 30 °C

Ratio	E_{corr} (mV_{SCE})	E_d (mV_{SCE})	I_{corr} (μA cm^{-2})	E (%)
[KI]/[4-MTH] = 0/10	−472	−430	527	65.8
[KI]/[4-MTH] = 3/7	−477	−409	485	68.5
[KI]/[4-MTH] = 5/5	−455	−400	191	87.6
[KI]/[4-MTH] = 7/3	−468	−398	277	82.0
[KI]/[4-MTH] = 10/0	−444	−375	554	64.0

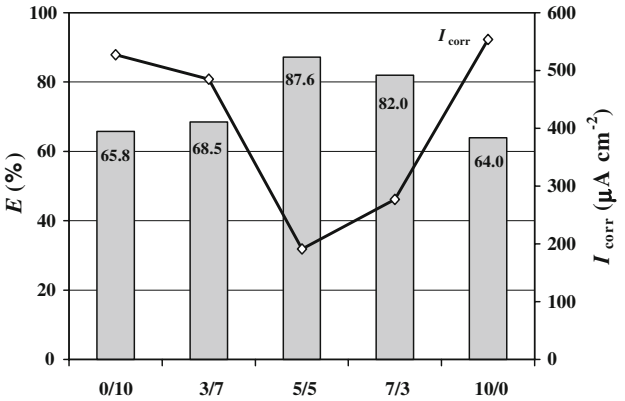

Fig. 8 Variation of I_{corr} and inhibition efficiency with ratio of [4-MTH]/[KI] for mild steel in 0.5 M H_2SO_4 containing 1×10^{-4} M of combined inhibitor (4-MTH + KI)

concentrations. The inhibition efficiency increased with increase in the combined inhibitor (4-MTH + KI) concentration. By comparing the corrosion rates in Tables 3, 4 and 6, it can be seen that the inhibitive properties of 4-MTH are greatly improved by the presence of KI. Taking the 1×10^{-4} M of 4-MTH, for example, the corrosion rate (I_{corr}) was 527 μA cm^{-2}, when only 4-MTH was used (Table 3). When both 4-MTH and KI were used together, the corresponding corrosion rate (I_{corr}) was decreased to 171 μA cm^{-2} (Table 6) and the E_d value was also increased from −430 mV_{SCE} (4-MTH alone) to −397 mV_{SCE} for the combined inhibitor. The iodide ions may compete with the 4-MTH molecules for adsorption on the metal surface, but the adsorbed iodide ions stabilize the adsorption of 4-MTH via electrostatic interaction so that the inhibition abilities of 4-MTH are improved by the combined use of 4-MTH and KI.

Table 6 The effect of total concentrations (4-MTH + KI) with ratio of [4-MTH]/[KI] = 5/5 on electrochemical parameters for mild steel in 0.5 M H_2SO_4 at 30 °C

4-MTH + KI conc. (M)	E_{corr} (mV_{SCE})	E_d (mV_{SCE})	I_{corr} (μA cm^{-2})	E (%)	S_θ
0.5×10^{-4}	−457	−416	343	77.7	1.66
1.0×10^{-4}	−455	−400	191	87.6	1.63
2.0×10^{-4}	−456	−397	171	88.9	1.11
3.0×10^{-4}	−441	−395	122	92.1	0.98

3.3 Adsorption isotherm

Assuming that the corrosion inhibition was caused by the adsorption of 4-MTH and KI, the degree of surface coverage (θ) for different concentrations was evaluated from Tafel polarization method using the following equation [51]:

$$\theta = \frac{I_{corr} - I_{corr(inh)}}{I_{corr}} \quad (1)$$

where I_{corr} and $I_{corr(inh)}$ are the corrosion current density values for uninhibited and inhibited samples, respectively.

The best correlation between the experimental results and isotherm functions was obtained using the Langmuir adsorption isotherm. The Langmuir isotherm for monolayer chemisorption is given by the following equation [52]:

$$\frac{C_{inh}}{\theta} = \frac{1}{K} + C_{inh} \quad (2)$$

where K is the equilibrium constant of the adsorption process. The plots of $C_{4\text{-MTH}}/\theta$, $\sim C_{4\text{-MTH}}$, $C_{KI}/\theta \sim C_{KI}$ and $C_{(4\text{-MTH+KI})}/\theta \sim C_{(4\text{-MTH+KI})}$ yield straight lines with nearly unit slope showing that the adsorption of these additives can be fitted to the Langmuir adsorption as presented in Fig. 9. It is found that all the linear correlation coefficients are very close to 1, clearly proving that the adsorption of 4-MTH, iodide ions, and the combined inhibitor (4-MTH + KI) from 0.5 M H_2SO_4 solutions on the mild steel obeys the Langmuir adsorption isotherm. The addition of KI does not change the adsorption behaviour of 4-MTH and Langmuir adsorption is also observed for mild steel in the solutions in the presence of the combined inhibitor (4-MTH + KI).

The synergistic effect of iodide ions with thiadiazole may be due to co-adsorption of I^- ions and 4-MTH molecules which may be both competitive and co-operative [53]. In competitive adsorption the anion and the 4-MTH molecule are adsorbed at different sites on the metal surface. In co-operative adsorption, the anion is chemisorbed on the surface and the cation is adsorbed on the anion layer. The extent of synergism between halide ions and 4-MTH

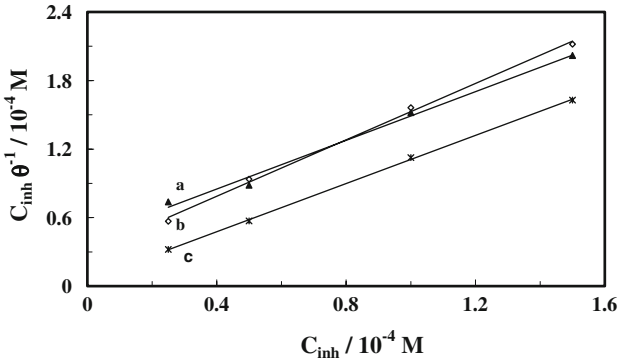

Fig. 9 Langmuir adsorption isotherm model of 4-MTH (a), KI (b) and combined inhibitor (4-MTH + KI) (c) on the mild steel electrode in 0.5 M H_2SO_4

has been analysed by estimating the synergism parameter (S_θ) obtained from the inhibition efficiency (from the Tafel polarization method) according to Aramaki and Hackerman [54] as:

$$S_\theta = \frac{1-\theta_{1+2}}{1-\theta'_{1+2}} \tag{3}$$

where $\theta_{1+2} = (\theta_1 + \theta_2) - (\theta_1\theta_2)$, θ_1 is the surface coverage by anions, θ_2 the surface coverage by cations and θ''_{1+2} is the measured surface coverage for cations in combination with anions.

Table 6 gives the computed values of S_θ which are found to be more than unity in most cases, thereby suggesting that the enhanced inhibition efficiency caused by the addition of iodide ions to 1,3,4-thiadiazole is only due to the synergistic effect. The synergistic inhibition effect in the present work can be explained as follows: The strong chemisorption of iodide ions on the metal surface is responsible for the synergistic effect of iodide ions in combination with the protonated species of the 4-MTH. These cations are then adsorbed by coulombic attraction on the metal surface where iodide ions are already adsorbed (cooperative adsorption) [54]. Stabilization of adsorbed iodide ions by means of electrostatic interaction with 4-MTH cations leads to greater surface coverage and thereby, greater inhibition.

4 Conclusions

2,5-Bis(4-methoxyphenyl)-1,3,4-thiadiazole (4-MTH) is shown to inhibit the corrosion of mild steel in 0.5 M H_2SO_4 and its inhibition action is due to the adsorption of 4-MTH molecules on the metal surface. In this case, the potential of desorption, E_d, remains nearly unchanged with increase in 4-MTH concentration. Addition of KI improves the $E(\%)$ of 4-MTH significantly and the high synergistic effect is clearly shown with an optimum mass ratio of [4-MTH]/[KI] = 5/5. The adsorption of 4-MTH is stabilised by the presence of iodide ions in the 0.5 M H_2SO_4 solutions. In this case, E_d values are sharply increased. Values of synergism parameter (S_θ) clearly show that the inhibition of corrosion by 4-MTH and iodide is synergistic by nature. Adsorption of 4-MTH alone and in combination with KI on the mild steel surface followed a Langmuir isotherm.

References

1. Khaled KF (2004) Appl Surf Sci 230:307
2. Branzoi V, Golgovici F, Branzoi F (2002) Mater Chem Phys 78:122
3. Algaber AS, El-Nemma EM, Saleh MM (2004) Mater Chem Phys 86:26
4. Migahed MA, Mohamed HM, Al-Sabagh AM (2003) Mater Chem Phys 80:169
5. Lashkari M, Arshadi MR (2004) Chem Phys 299:131
6. Popova A, Christov M, Raicheva S, Sokolova E (2004) Corros Sci 46:1333
7. Mu GN, Li XM, Li F (2004) Mater Chem Phys 86:59
8. Li XM, Tang LB (2005) Mater Chem Phys 90:286
9. Ebenso EE (2003) Mater Chem Phys 79:58
10. Hosseini M, Mertens SFL, Arshadi MR (2003) Corros Sci 45:1473
11. Rajendran S, Apparao BV, Palaniswamy N (1998) Electrochim Acta 44:533
12. Feng Y, Siow KS, Teo WK, Hsieh AK (1999) Corros Sci 41:829
13. Mu GN, Li XM, Liu GH (2005) Corros Sci 47:1932
14. Li XM, Tang LB, Li L, Mu GN, Liu GH (2006) Corros Sci 48:308
15. Atia AA, Saleh MM (2003) J Appl Electrochem 33:171
16. Ochoa N, Moran F, Pébère N (2004) J Appl Electrochem 34:487
17. Bentiss F, Traisnel M, Chaibi N, Mernari B, Vezin H, Lagrenée M (2002) Corros Sci 44:2271
18. El Azhar M, Mernari B, Traisnel M, Bentiss F, Lagrenée M (2001) Corros Sci 43:2229
19. Lagrenée M, Mernari B, Bouanis M, Traisnel M, Bentiss F (2002) Corros Sci 44:573
20. Abd El-Maksoud SA (2003) Appl Surf Sci 206:129
21. Elkadi L, Mernari B, Traisnel M, Bentiss F, Lagrenée M (2000) Corros Sci 42:703
22. Bentiss F, Traisnel M, Lagrenée M (2000) Br Corros J 35:315
23. Lebrini M, Bentiss F, Lagrenée M (2005) J. Heterocycl Chem 42:991
24. Bentiss F, Lagrenée M, Traisnel M, Hornez JC (1999) Corrosion 55:968
25. McCafferty E, Pravdic V, Zettlemoyer AC (1999) Trans Faraday Soc 66:237
26. Olivares O, Likhanova NV, Gómez B, Navarrete J, Llanos-Serrano ME, Arce E, Hallen JM (2006) Appl Surf Sci 252:2894
27. Bentiss F, Lebrini M, Lagrenée M, Traisnel M, Elfarouk A, Vezin H (2008) Electrochim Acta 52:6865
28. Murakawa T, Hackerman N (1964) Corros Sci 4:387
29. Allabergenov KD, Kurbanov FK (1979) Zashch Met 15:472
30. Rengamati S, Muralidharan S, Anbu Kulandainathan M, Venkatakrishna Iyer S (1994) J Appl Electrochem 24:355
31. JO'M Bockris, Yang B (1991) J Electrochem Soc 135:2237

32. Bentiss F, Traisnel M, Lagrenée M (2001) J Appl Electrochem 31:41
33. Kertit S, Hammouti B (1996) Appl Surf Sci 93:59
34. Popova A, Raicheva S, Sokolova E, Christov M (1996) Langmuir 12:1083
35. Lebrini M, Lagrenée M, Vezin H, Traisnel M, Bentiss F (2007) Corros Sci 49:2254
36. MacCafferty E (1997) Corros Sci 39:243
37. Bentiss F, Lebrini M, Lagrenée M (2005) Corros Sci 4:2915
38. Bartos M, Hackerman N (1992) J Electrochem Soc 139:3428
39. MacFarlane DR, Smedley SI (1986) J Electrochem Soc 133:2240
40. Bentiss F, Bouanis M, Mernari B, Traisnel M, Lagrenée M (2002) J Appl Electrochem 32:671
41. Heusler KE, Cartledge GH (1961) J Electrochem Soc 108:732
42. Çalışkan N, Bilgiç S (2000) Appl Surf Sci 153:128
43. Iofa ZA, Batrakov VV, Cho-Ngok-Ba (1964) Electrochim Acta 9:1645
44. Antropov AI, Makushin EM, Panasenko VP (1981) Inhibitors of metal corrosion. Tekhnika, Kiev
45. Iofa ZA (1965) In: Proceeding of the 2nd European symposium on corrosion inhibitors, Ferrara 151
46. McCafferty E (1979) Corrosion control by coatings. Science Press, Princeton
47. Brummer SB, Makrides AC (1964) J Phys Chem 68:1448
48. Lebrini M, Lagrenée M, Vezin H, Gengembre L, Bentiss F (2005) Corros Sci 47:485
49. Antropov LI (1963) J Phys Chem 37:965
50. Bartos M, Kapusta SD, Hackerman N (1993) J Electrochem Soc 140:2604
51. Khamis E (1990) Corrosion 46:6
52. Agrawal R, Namboodhiri TKG (1990) Corros Sci 30:37
53. Schmitt G, Bedbur K (1985) Werkst Korros 36:273
54. Aramaki K, Hackerman N (1969) J Electrochem Soc 116:568